AIAA JOURNAL
Vol. 39, No. 6, June 2001

Numerical Study of Supersonic, Underwater Flows past a Blunt Body

S. M. Liang,* C. T. Chen,† and H. Chen‡
National Cheng-Kung University, Tainan 701, Taiwan, Republic of China

Supersonic flows past a blunt body in air and in water are numerically investigated by using a high-resolution Euler/Navier–Stokes solver. The numerical method used is a fourth-order Runge–Kutta method for time integration with a fifth-order weighted essentially nonoscillatory scheme for discretizing the convective terms and central differencing for the viscous terms. The inviscid- and viscous-flow results are compared. It was found that the inviscid-flow model is able to predict reasonably accurate flowfields such as the bow shock and sonic-line locations. Moreover, for the case of medium water the bow-shock location is farther upstream, and the sonic line is farther downstream compared with the case of medium air.

Introduction

THE problem of supersonic flows past blunt bodies in water has academic interest and practical applications. Supersonic, underwater flows can have different dynamic features from the supersonic aerodynamics and are less well known. The problem originated from a high-speed steel jet in an explosive charge.[1] This high-speed jet resulted from the passage of a blast wave through the explosive and the steel liner in the explosive charge. The jet velocity can be as high as 10,000 m/s. In the past literature Hsieh[2] used an implicit, approximately factored finite difference algorithm of Beam and Warming[3] for solving the axisymmetric Euler equations associated with a simplified Tait equation. However, Hsieh's result seemed to be inaccurate. In this study a high-order algorithm[4] of a fourth-order Runge–Kutta time integration method and a fifth-order WENO (weighted essentially nonoscillatory) scheme of Jiang and Shu[5] for discretizing the convective terms is used. Moreover, instead of the simplified Tait equation, the modified Tait equation[6] is employed. The simplified and modified Tait equations will be described in the next section. The objective of this study is to accurately predict the supersonic, underwater flowfield around a blunt body by using the high-order algorithm.

Mathematical Formulation and Numerical Method

Governing Equations

Assume that there are no effects from bubbles in the water flow. The governing equations for the supersonic, underwater flow are the continuity, momentum, and energy equations. In the Cartesian coordinates they can be written in a conservation form as

$$\frac{\partial Q}{\partial t}+\frac{\partial F}{\partial x}+\frac{\partial G}{\partial y}+H=\frac{\partial F_v}{\partial x}+\frac{\partial G_v}{\partial y}+H_v \qquad (1)$$

where $Q=[\rho, \rho u, \rho v, E]^t$ is the conserved variables; F and G the flux vectors; and H the source term caused by axisymmetry; ρ the density; $p(=p'-B)$ the pressure; u and v the velocity components; c the speed of sound; E the total energy per unit volume; p' the modified pressure; and B a constant. In this study B is chosen to be 2955 bar for water and zero for air. The subscript v denotes the terms caused by the flow viscosity. The modified pressure p' is related to the flow variables E, u, v:

$$E=p'/(\gamma-1)+\rho(u^2+v^2)/2$$

where the value of γ is chosen as 7.44 for water and 1.4 for air. The equation of state for water is described by the modified Tait equation[6] defined as

$$\rho(p,T)=\rho(0,T)(1+p/B)^{1/\gamma}$$

with the assumption of $\rho(0, T)$ being a constant for 273 K < T < 333 K. Sometimes, the modified Tait equation is further simplified:

$$\rho(p,T)=\rho(0,T)(p/B)^{1/\gamma}$$

For a flow of air, the temperature can be computed from the equation of state once the pressure and the density are known. For a water flow the temperature is computed based on the data from the steam tables in Ref. 7. Namely,

$$T=T_0+\beta_s(p-p_0), \qquad \beta_s\equiv\left(\frac{\partial T}{\partial p}\right)_s$$

where β_s is the isentropic temperature-pressure coefficient and T_0 and p_0 are the freestream temperature and pressure, respectively. Moreover, the flow variables (ρ, u, v, p, E) and the independent variables (x, y, t) can be properly nondimensionalized by using the freestream condition. We chose the characteristic length to be the nose radius of the body. For easy treatment of boundary conditions, the governing equations are usually written in a body-fitted coordinate.

Numerical Method

The numerical method of high-order accuracy in a finite volume approach is used to solve Eq. (1). This method consists of a fourth-order Runge–Kutta method for time integration and a fifth-order WENO scheme[5] for discretizing the convective terms. Moreover, the central difference of second-order accuracy is used for the viscous terms. The Courant number is set to be 0.6 for all steady flow calculations. All computations were performed on a personal computer, Pentium II-266, with a 256-MB memory.

Initial and Boundary Conditions

The physical domain used, as shown in Fig. 1, is mapped into a rectangular region in the computational domain. At the inlet the boundary condition is the given freestream condition. At the symmetric axis a symmetry condition is imposed. At the outlet a first-order linear extrapolation for flow variables is used. On the body surface the no-slip boundary condition is prescribed, and an adiabatic wall is also assumed. The initial condition is a quiet flow everywhere except for the inlet where the flow condition is given.

Results and Discussion

Code Validation

The computer program developed is validated on a nozzle[7] with the area ratios of $A_i/A_t=9.76$ and $A_e/A_t=9$ because there are

Received 27 March 2000; revision received 24 October 2000; accepted for publication 22 November 2000.

*Professor, Institute of Aeronautics and Astronautics. Associate Fellow AIAA.
†Graduate Student; currently Engineer of Automotive Research and Testing Center, Hu-Kou Hsiang, Hsing-Chu Hsien 303, Taiwan, Republic of China.
‡Ph.D. Student, Institute of Aeronautics and Astronautics.

experimental data and numerical results for comparison, where A_i, A_e, A_t denote the nozzle cross-sectional areas at the inlet, the exit, and the throat, respectively. The fluid is air. The Reynolds number is chosen to be 1.8×10^6. Figure 2 shows the computed result. Figure 2a depicts the dimensionless pressure distribution along the nozzle wall and the symmetric axis, respectively. Figure 2b shows the Mach-number distribution along the symmetric axis. From Fig. 2, one can see that very good agreement is obtained by comparing the present result with the experimental data[8] and the existing numerical data[9] obtained by the implicit total variation diminishing (TVD) scheme.[10]

The computer program is also verified on the problem of a simple one-dimensional underwater shock-wave reflection problem. The initial shock wave has a pressure ratio of 700 with the shock Mach number of 1.063. After shock-wave reflection from the end, the computed pressure ratio for the reflected shock is 2.122. The analytic pressure ratio for the reflected shock is 2.119. The relative error is only 0.033%.

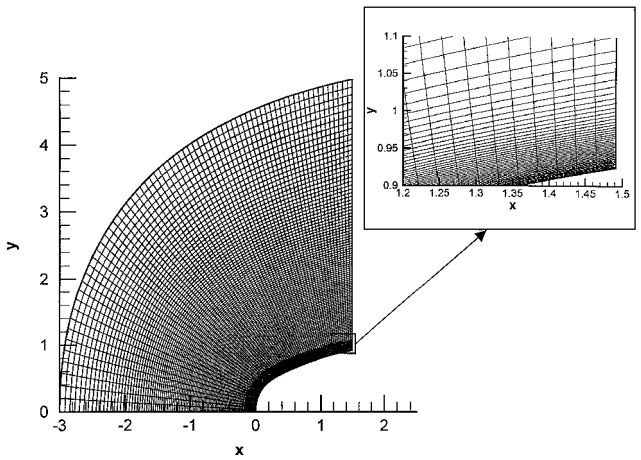

Fig. 1 Computational grid of 141 × 71 grid points with a subplot for the viscous flow calculation.

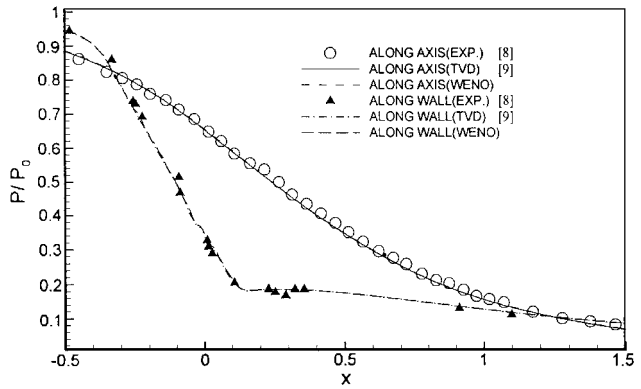

a) Pressure

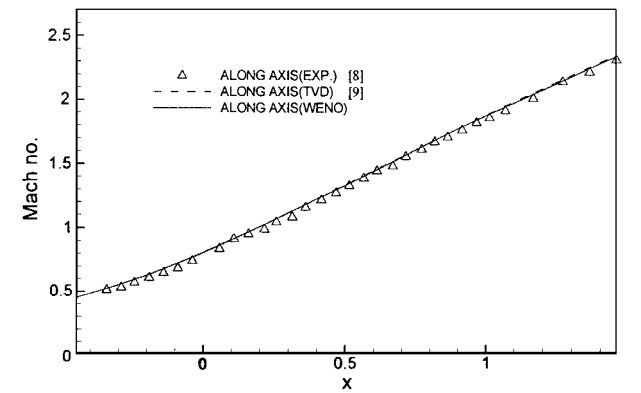

b) Mach number

Fig. 2 Comparison of the computed result with the experimental data and the existing numerical result.

Supersonic, Underwater Flow Problem

A blunt body with a parabola-like shape is considered,[11] as shown in Fig. 1. The nose radius is assumed to be unity. The effect of the number of grid points on solution accuracy was studied by using the inviscid-flow model. The grid independence study was made by using five grids: 51×31 (grid 1), 71×41 (grid 2), 101×61 (grid 3), 141×91 (grid 4), and 181×121 (grid 5). The improvement of grid refinement on the dimensionless surface (modified) pressure at the point $s = 1.01$ was found to be 6, 20, 4.4, and 3.3%, respectively, when grid i is refined to grid $i+1$, $i = 1, 2, 3, 4$. Here s denotes the distance along the body surface and is measured from the nose. Because the improvement of grid refinement from grid 4 to 5 is not significant, the 101×61 grid is used for later study in order to save computational time. The reader can refer to Fig. 1. For the viscous flow calculation, near the body surface additional 40 grid points in the normal direction and 10 grid points in the circumferential direction are added to the original 101×61 grid, as shown in Fig. 1. These 40 grid points are enough to resolve the boundary layer. The smallest grid size close to the body surface in the normal direction is 10^{-4}. A subplot is included to show the stretched grid points near the surface. The Reynolds number is chosen to be 10^4. The Prandtl number for water is seven.

Figure 3 shows the calculated results using the viscous- and inviscid-flow models at $M = 3$. Figure 3a shows the Mach-number

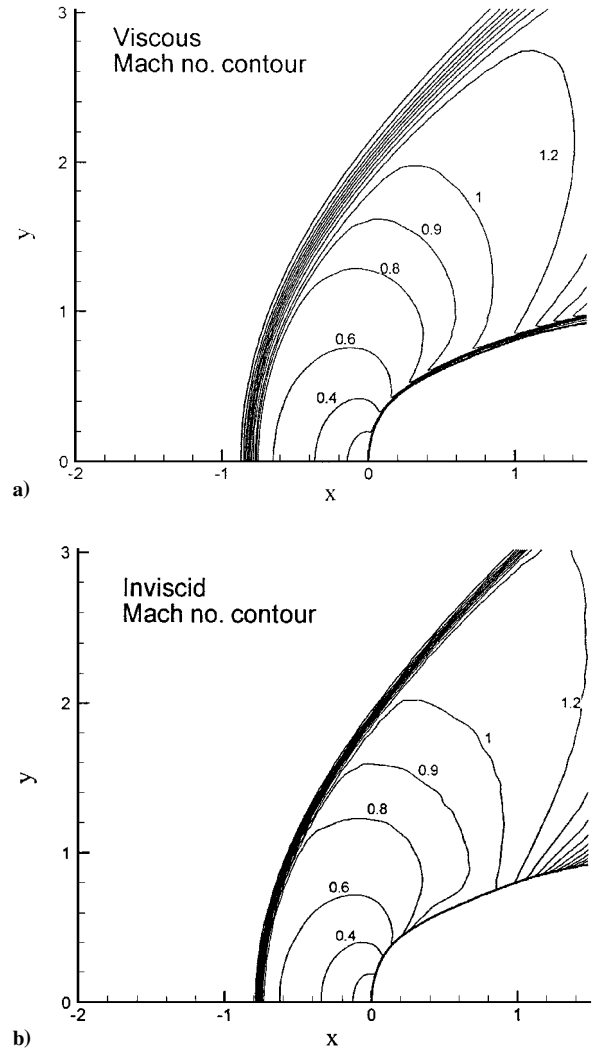

a)

b)

Fig. 3 Computed Mach-number distributions using viscous- and inviscid-flow models: $M = 3$.

distribution of the viscous model and Fig. 3b for the inviscid-flow model. The sonic line is indicated by $M = 1$. Basically, no large deviation in the Mach contours occurs for either result except in the vicinity of the body surface and of the shock wave. The shock-wave locations for both flow models are very close. Obviously, the shock-wave representation for the inviscid flow is sharper than that for the viscous flow. The same situation occurred for the pressure distribution for both flow models.

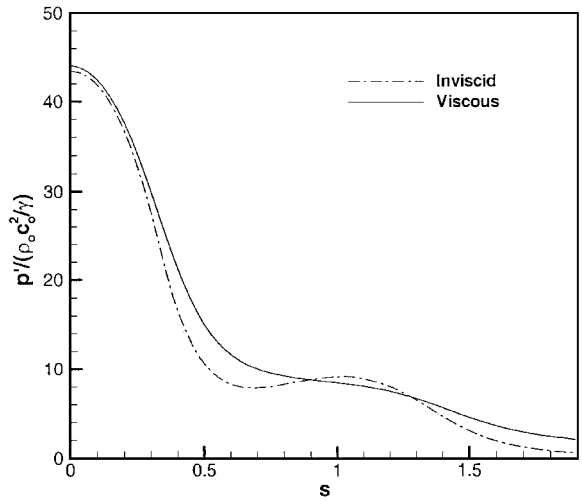

Fig. 4 Comparison of the computed surface pressure distributions with Hsieh's result: $M = 3$.

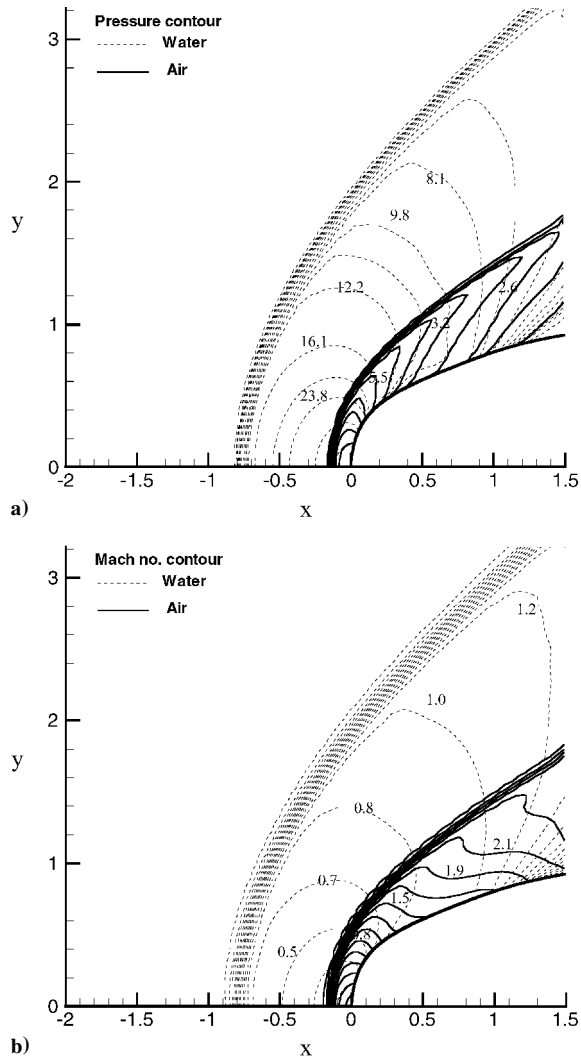

Fig. 5 Comparison of the a) pressure and b) Mach-number distributions for air and water flows: $M = 3$.

Figure 4 shows the modified pressure distributions along the body surface. The pressure is normalized by $\rho_0 c_0^2/\gamma$. Here ρ_0, c_0 denote the density and the sound speed $[c = \sqrt{(\gamma p'/\rho)}]$ at the freestream condition. We have compared our result of surface pressure distribution with Hsieh's result. Our result is more accurate than Hsieh's prediction. In the inviscid-flow model the predicted dimensionless stagnation pressures are 43.4 for the inviscid model and 44.1 for the viscous model. The analytic value is 42.8. The relative errors of the predicted stagnation pressures are 1.4 and 3%, respectively. There is an oscillation on the inviscid surface pressure, resulting in a local minimum at $s = 0.7$ and a local maximum $s = 1$. For the viscous model there is no oscillation because of the boundary-layer effect, resulting in a monotonic surface pressure distribution. The largest deviation between these two results occurs at about $s = 0.5$. The computation time for the viscous-flow calculation is approximately 30 times longer than that for the inviscid-flow calculation.

Because the Mach-number distributions obtained by the viscous- and inviscid-flow models are almost the same outside the boundary layer, only the inviscid-flow model is considered for comparison of the water flowfield with the airflow field. Figure 5 shows the comparison of the pressure and Mach-number distributions in air and in water at $M = 3$. The distinguished features of the water flowfield are the locations of the shock wave and the sonic line, which are quite different from those for the airflow. Because the compressibility of air is larger than that for the water, the bow shock in water is located farther upstream, and the sonic line is located farther downstream, compared with those for the airflow. For the inviscid model the surface pressure decreased more rapidly with the distance from the stagnation point than that for the viscous model. The dimensionless stagnation pressure in the water flow is 43.4, which is about 3.6 times larger than that (11.9) for the air. Assume the incoming flow is at a room temperature (20°C). The stagnation temperature was found to be 360°C with a vaporized pressure of 186.5 bar.[11] The corresponding dimensionless vaporized pressure is about 0.062, which is much less than the value of 43.4. Therefore, no vaporization would occur near the stagnation point.

Conclusions

A high-order algorithm has been developed and used to investigate the supersonic underwater flow past a blunt body. The computer program is validated to be reasonably accurate. It is found that the viscous-flow model predicts better surface pressures than the inviscid model. Generally speaking, the inviscid model can be used to predict reasonably accurate flowfields such as the locations of the bow shock and the sonic line. The supersonic flowfields in water and in air at Mach 3 are computed and compared. The bow shock is located farther upstream for the water case than that for the air case. Consequently, the sonic line is located farther downstream for the water case than that for the air case.

Acknowledgment

The support for this study by the National Science Council under Contract NSC 89-2612-E-006-018 is gratefully acknowledged.

References

[1]Birkhoff, G., MacDougall, D. P., Pugh, E. M., and Sir Taylor, G., "Explosive with Lined Cavities," *Journal of Applied Physics*, Vol. 19, No. 6, 1948, pp. 563–582.

[2]Hsieh, T., "Supersonic Flow over Blunt Bodies in Water—A Preliminary Study," AIAA Paper 84-1643, June 1984.

[3]Beam, R. M., and Warming, R. F., "An Implicit Factored Scheme for the Compressible Navier-Stokes Equations," *AIAA Journal*, Vol. 16, No. 4, 1978, pp. 393–402.

[4]Liang, S. M., and Chen, H., "Numerical Simulation of Underwater Blast-Wave Focusing Using a High-Order Scheme," *AIAA Journal*, Vol. 37, No. 8, 1999, pp. 1010–1013.

[5]Jiang, G. S., and Shu, C. W., "Efficient Implementation of Weighted ENO Scheme," *Journal of Computational Physics*, Vol. 126, No. 1, 1996, pp. 202–228.

[6]Sommerfeld, M., and Müller, H. M., "Experimental and Numerical

Studies of Shock Wave Focusing in Water," *Experiments in Fluids*, Vol. 6, No. 3, 1988, pp. 209–216.

[7]Haar, L., Gallagher, J. S., and Kell, G. S., *NBS/CRC Steam Tables*, Hemisphere, Washington, DC, 1984, p. 260.

[8]Back, L. H., Massier, P. F., and Gier, H. L., "Comparison of Measured and Predicted Flows Through Conical Supersonic Nozzle, with Emphasis on the Transonic Region," *AIAA Journal*, Vol. 3, No. 9, 1965, pp. 1606–1614.

[9]Hwang, K. L., "Numerical Investigation of Nozzle Flow Field in the Thruster of Satellites," M.S. Thesis, Inst. of Aeronautics and Astronautics, National Cheng-Kung Univ., Tainan, Taiwan, ROC, June 1995.

[10]Yee, H. C., and Harten, A., "Implicit TVD Schemes for Hypersonic Conservation Laws in Curvilinear Coordinates," *AIAA Journal*, Vol. 25, No. 2, 1987, pp. 266–274.

[11]Chen, C. T., "Numerical Study of Supersonic Flows over Blunt Bodies in Water," M.S. Thesis, Inst. of Aeronautics and Astronautics, National Cheng-Kung Univ., Tainan, Taiwan, ROC, June 1999.

K. Kailasanath
Associate Editor